

# AUTOMATIC IMAGE SEGMENTATION WITH ANISOTROPIC FAST MARCHING ALGORITHM AND GEODESIC VOTING

Vijaya K. Ghorpade and Laurent D. Cohen

CEREMADE, UMR 7534, Université Paris Dauphine, 75775 Paris Cedex 16, France

## ABSTRACT

Segmentation methods based on energy minimization techniques like geodesic active contour model generally needs manual intervention to provide initial points to calculate minimal paths. In this paper, we propose complete automation of segmentation. Seeds and Tips are automatically detected, and geodesics are calculated using Anisotropic Fast Marching algorithm. Fast Marching algorithm computes in a single pass, the evolution of the front, at a speed locally given by its position. Anisotropic Fast Marching (AFM) is a variant of Fast Marching, in which the the measure of path length (and the front speed) depends not only on the path position, but also on path direction and orientation. In this work, a gradient based metric has been defined and AFM is evaluated iteratively over a set of points which are automatically detected on the object boundary. Geodesic voting is then applied to get the segmented structure.

*Index terms*— Segmentation, Anisotropic Fast Marching algorithm, Geodesic voting, Riemannian metric.

## 1. INTRODUCTION

Energy minimization techniques have been widely applied to solve various problems in image processing and computer vision. Minimal paths [1] based segmentation is very powerful and robust against noisy images and have the added advantage of global minimizers. Vessel tree structure extraction is trademark application of this method [2]. Although it has many advantages, complete automatic segmentation is still a challenging task, as it needs at least one user/manual input. In this paper, a novel approach has been proposed for automatic segmentation of natural images. This paper describes/focuses on three main important techniques/aspects of the approach: firstly, on the algorithm which computes the front evolution itself; secondly, the algorithmic details of automatically detecting Seeds and Tips; thirdly it focuses on removing the erroneous bridges between parallel edges.

## 2. BACKGROUND

### 2.1. Minimal path model

Given a 2D image  $I : \Omega \rightarrow \mathbf{R}^+$  and two points  $\mathbf{p}_1$  and  $\mathbf{p}_2$ , a crucial step of the minimal paths [1] is to build a potential  $\mathcal{P} : \Omega \rightarrow \mathbf{R}^+$  with lower values near the features. The minimal paths model is formulated to find geodesic paths  $\gamma$  to minimize the following energy functional  $E : \mathcal{A}_{\mathbf{p}_1, \mathbf{p}_2} \rightarrow \mathbf{R}^+$ :

$$E(\gamma) = \int_{\gamma} (\mathcal{P}(\gamma) + w) ds = \int_{\gamma} \tilde{\mathcal{P}}(\gamma) ds \quad (1)$$

Where  $\mathcal{A}_{\mathbf{p}_1, \mathbf{p}_2}$  is the set of all paths linking  $\mathbf{p}_1$  and  $\mathbf{p}_2$ ,  $s$  is the arc-length parameter and  $w$  is a positive constant. A minimal path can be defined as a curve connecting  $\mathbf{p}_1$  and  $\mathbf{p}_2$  that globally minimizes the energy (1). The solution of this optimization problem is obtained through the computation of the minimal action map  $\mathcal{U} : \Omega \rightarrow \mathbf{R}^+$ . The minimal action map is the minimal energy integrated along a path between  $\mathbf{p}_1$  and any point  $\mathbf{x}$  of the domain  $\Omega$ :

$$\mathcal{U}(\mathbf{x}) = \min_{\gamma \in \mathcal{A}_{\mathbf{p}_1, \mathbf{x}}} \int_{\gamma} \tilde{\mathcal{P}}(\gamma) ds, \quad \forall \mathbf{x} \in \Omega \quad (2)$$

And  $\mathcal{U}$  satisfies the Eikonal equation:

$$\begin{cases} \|\nabla \mathcal{U}\| = \tilde{\mathcal{P}}(\gamma) & \forall \mathbf{x} \in \Omega \\ \mathcal{U}(\mathbf{p}_1) = 0 \end{cases} \quad (3)$$

The Fast Marching Algorithm (FMM) [3] [4] can be adapted to solve this Eikonal equation and compute the evolution of the front. The shortest path or minimal geodesic, joining an arbitrary point  $\mathbf{p}_2$ , to the front source  $\mathbf{p}_1$  can then be extracted by a gradient descent on the image of front arrival times. Minimal geodesic paths were used extensively for interactive segmentation (ref [5]). Also some work used a set of minimal paths to get a more complete segmentation [6] [7].

### 2.2. Anisotropic Fast Marching Algorithm (AFM)

AFM is an efficient method used for computation of *shortest paths* or *geodesics* within a domain  $\Omega \subset \mathbb{R}^d$ . It is a variant of FMM, as the measure of path length (and the front speed)

depends not only on the path position, but also on the path direction and orientation [8]. Path length is measured locally via a metric:  $\mathcal{F}$ , which associates to each point  $z \in \Omega$  a norm  $\mathcal{F}_z$  on  $\mathbb{R}^d$ . The length of a smooth path  $\gamma : [0, 1] \rightarrow \Omega$  is

$$\text{Length}(\gamma) := \int_0^1 \mathcal{F}_{\gamma(t)}(\gamma'(t)) dt. \quad (4)$$

The distance between two points  $\mathbf{p}_1, \mathbf{p}_2 \in \Omega$  is defined as the length of the shortest path joining these points:

$$D(\mathbf{p}_1, \mathbf{p}_2) := \inf\{\text{Length}(\gamma); \gamma : [0, 1] \rightarrow \Omega, \gamma(0) = \mathbf{p}_1, \gamma(1) = \mathbf{p}_2\}. \quad (5)$$

AFM algorithm allows to estimate the map  $D(x_0, \cdot) : \Omega \rightarrow \mathbb{R}_+$  of distances from a given Seed  $x_0 \in \Omega$  to any other point, and to extract the corresponding shortest paths. It can take Riemannian or Finsler metrics as input, which are potentially anisotropic and asymmetric [9] [10]

$$\mathcal{F}_z(u) = \sqrt{\langle u, M(z)u \rangle}, \quad (\text{Riemannian Metric})$$

$$\mathcal{F}_z(u) = \sqrt{\langle u, M(z)u \rangle} - \langle \omega(z), u \rangle. \quad (\text{Finsler Metric})$$

Riemannian metrics are defined through a field  $M : \Omega \rightarrow S_d^+$  of symmetric positive definite matrices. The implemented family of asymmetric Finsler metrics, involves in addition a vector field  $\omega : \Omega \rightarrow \mathbb{R}^d$  [10].

### 3. APPROACH

#### 3.1. Scooping

In an image  $I : \Omega \rightarrow \mathbf{R}^+$  of an object  $\Omega_0 \subset \Omega$ , the image gradient of  $I$ :  $V(z) = \nabla I(z) = [\frac{\partial I}{\partial x}, \frac{\partial I}{\partial y}]^T$  is strong on the object boundary  $\partial\Omega_0$ , and points outwards of it. A speed function  $s(z) := 1 + \|V(z)\|^\alpha$  (for some parameter  $\alpha > 0$ ) is defined, which takes higher values at positions having larger gradient magnitude. A gradient based Riemannian Metric  $M(z)$  [9]

$$M(z) := \frac{\text{Id}_2}{s(z)^2} + \left(1 - \frac{1}{s(z)^2}\right) \frac{V(z)V(z)^T}{\|V(z)\|^2}. \quad (6)$$

is made in such a way that it prescribes the path speed  $s(z)$  in the direction orthogonal to  $V(z)$ , hence *tangentially* to the object boundary  $\partial\Omega_0$ : Anisotropic Fast Marching basically takes Metric ( $M(z)$ ), Seeds and Tips as Input. These Seeds and Tips are usually given manually on the GUI or hard-coded. In our paper, we propose a method to automatically detect these points. We define this process as *Scooping*, as in each iteration of AFM, a circular region in the image having interest points are scooped out. All the pixels(points) whose gradient magnitude:  $|\nabla I(z)| = \sqrt{\left(\frac{\partial I}{\partial x}\right)^2 + \left(\frac{\partial I}{\partial y}\right)^2}$  greater than certain threshold  $T$ , are considered to be in the set of potential points  $P$ . Each point

$p_i \in P$  is considered as start (Seed) point for AFM. And, all the points( $p^r$ ) within certain radius  $r$ , are taken as Tips for  $p_i$ . The object boundary between two points (a Seed( $p_i$ ) and a Tip( $p_k^r$ ), where  $0 \leq k \leq n$  and  $n$  is the number of points in the region  $r$ )  $\in \partial\Omega_0$  is then extracted by AFM as the shortest path between these points with respect to the Anisotropic metric of speed function  $s(z)$  [9]. In each execution of AFM, all geodesics are extracted between the Seed and Tips.

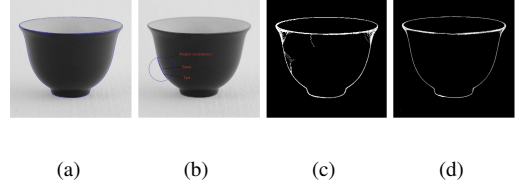


Figure 1: Scooping and Geodesic Voting. (a) Object with all the points  $P$  (b) Scooped part having Seed, Tips and region of interest (c) Geodesic density with no threshold (d) with threshold 10 (see text).

#### 3.2. Geodesic Voting

AFM is run iteratively over all the points in  $P$ , resulting in a set of minimal paths  $y_k$  for each execution. Each path of  $y_k$  for each iteration of AFM is then analysed and a voting scheme is applied (for details of Geodesic voting, refer [2][11][12][13]). When backtracking each path, 1 is added to each pixel we pass over in the image domain. At the end of this process, pixels on the boundary of the object will have high vote, since many paths pass over it. On the contrary, pixels in the background will generally have a low vote since very few paths pass over them. The result of this voting scheme is called the geodesic density [2]. This means at each pixel the density of geodesics that pass over this pixel. The segmented structure correspond to the points with high geodesic density. We define the voting score or the geodesic density at each pixel  $p$  of the image by:

$$\mu(p) = \sum_{i=1}^n \delta_p(y_k) \quad (7)$$

where the function  $\delta_p(y)$  returns 1 if the path  $y$  crosses the pixel  $p$ , else 0. Once the geodesic voting is made the object structure is obtained by a simple threshold on geodesic density  $\mu$  (see Figure 1).

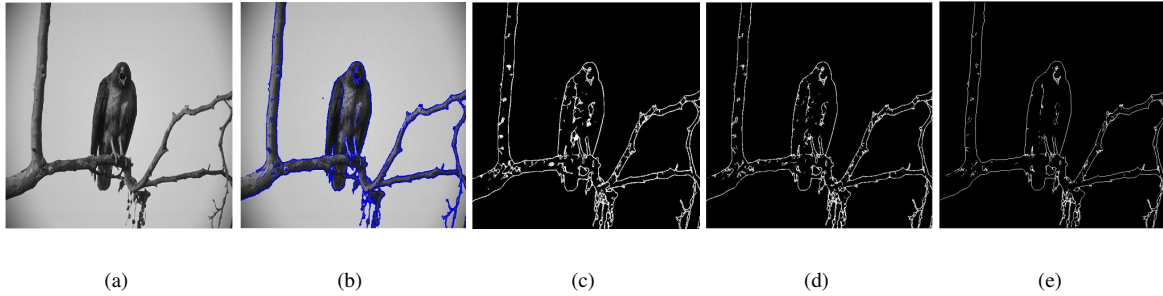


Figure 2: AFM Early abort case 2. (a) original image (b) all points  $P$  (c) geodesic density with no threshold (d) with 10 threshold (e) with 50 threshold

#### 4. EARLY ABORT AFM: FRONT TERMINATION APPROACH

Anisotropic Fast Marching algorithm estimates the distances  $D(x_0, \cdot)$  for the entire image domain in a single pass, with approximate complexity  $\mathcal{O}(N \ln N)$ , where  $N$  denotes the cardinality of the discrete domain [9].

Executing it iteratively for all the points is not only redundant but also very computationally expensive and time consuming. In order to reduce the computation time, we have proposed an early abort mechanism which not only reduces the time but also avoids the bridges between the parallel edges. A two different abort systems have been implemented, both of them limits the front propagation within the radius region  $r$ .

1. Early abort: All Tips reached
2. Early abort: First Tip at  $r$  reached.

##### 4.1. Early abort: All Tips reached

In this approach, the front propagation is terminated when all the Tips ( $p_r$ ) within radius  $r$  are reached from the source  $p_i$ . The elapsed time for one complete pass for this approach has been reduced by one-third (from 925.76 seconds to 299.15 seconds). The AFM in this case takes an additional group of boundary points on the circle, at which it stops.

##### 4.2. Early abort: First Tip at $r$ reached

The first approach is fast, but as geodesics are extracted locally within a region, it leads to bridges in case of parallel edges as can be seen in Figure 4 (Top). The front propagated from the source point by AFM actually progresses in elliptical shape, with velocity  $(1/\tilde{P})$ , where  $\int_{\gamma} \tilde{P}$  is geodesic active contour energy, and  $\gamma$  is the path joining the two points. As a result, equidistant points within  $r$  from the source are

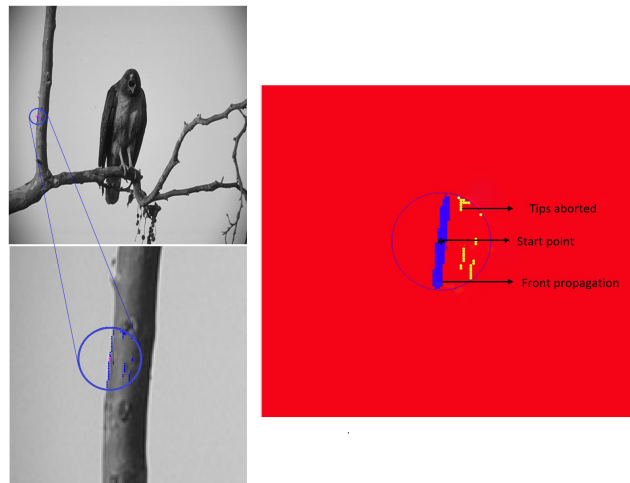
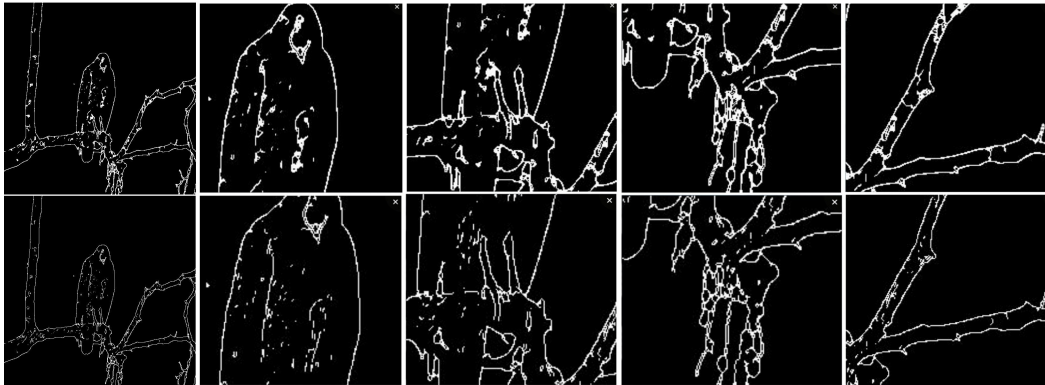


Figure 3: AFM early abort: yellow points on the parallel edge are not reached as the front terminates when it reaches the first Tip at radius  $r$ .

reached at different times. Eventually, the Tips on the parallel edges are reached almost at the last. Based on this behaviour of the front propagation, a second approach is proposed where the front is aborted well before they reach the Tips on the parallel edges (see Figure 3 and Figure 2). Here the AFM aborts when the first boundary point at radius  $r$  is reached. As a result the computation time is also decreased compared to case 1. The comparison of the results from both methods are shown in the Figure 4, where the images on the top are from the first approach and below are from second approach.

## 5. EXPERIMENTS

The binary image generated as a result of geodesic voting process shows the segmented structure of the object in the image. The quality of the structure extracted varies, if the



(a)

Figure 4: Comparison of two approaches of AFM early abort(see text). It is clearly seen that bridges between parallel edges are removed in bottom figures.

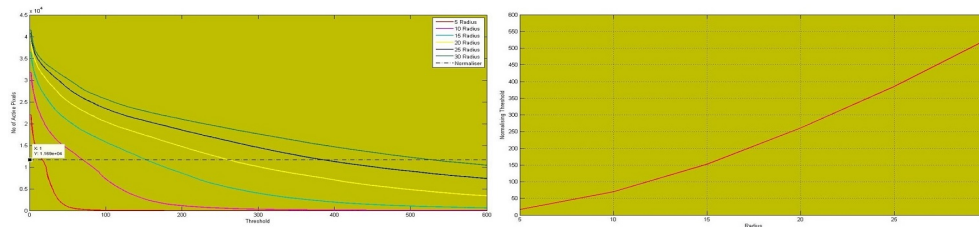


Figure 5: (Left) Threshold vs number of active pixels for different radii. (Right) Calibration curve

threshold on the geodesic density is increased it leads to an increasing number of active pixels (remaining pixels left after a threshold on geodesic density). The quality of the segmentation also depends on the radii  $r$  considered, the larger the radius the better the gaps are covered, but also leads to false structures protruding from the object at lower geodesic density threshold. The smaller the radius the better the bridges are avoided but at the cost of breaks in the structure at higher geodesic density threshold. A trade-off is obtained using a calibration curve to get the best quality structure threshold at any given arbitrary radius. This calibration curve is obtained by finding a normalizing threshold for few different discrete radius values resulting in the same number of active pixels ( $\approx P$ , the total number of potential points left after a gradient magnitude threshold ( $T$ ) on original image domain) (see Figure 5). Calibration curve augments automation of segmentation to even find the possible best segmented structure.

## 6. CONSLUSION AND FUTURE WORK

In this paper we have presented a novel way of image segmentation using Anisotropic Fast Marching algorithm with-

out any manual intervention. We have also improvised AFM to decrease speed of computation and also remove false bridges between parallel edges, a calibration curve is made to find the best possible parameters for better quality of segmentation. We focus on defining metrics to evaluate and compare the quality of segmentation with other state-of-the art and classical methods using gold standard datasets in future work.

## Acknowledgement

The authors would like to thank Dr. Jean-Marie Mirebeau for providing the AFM algorithm, and for the fruitful discussions about this work.

## 7. REFERENCES

- [1] L. D. Cohen and R. Kimmel, "Global minimum for active contour models: A minimal path approach," *International Journal of Computer Vision*, vol. 24, no. 1, pp. 57–78, Aug. 1997.

- [2] Y. Rouchdy and L. D. Cohen, "A geodesic voting method for the segmentation of tubular tree and centerlines," in *Proceedings of the 8th IEEE International Symposium on Biomedical Imaging: From Nano to Macro, ISBI 2011, March 30 - April 2, 2011, Chicago, Illinois, USA*, 2011, pp. 979–983.
- [3] J. N. Tsitsiklis, "Efficient algorithms for globally optimal trajectories," *IEEE Transactions on Automatic Control*, vol. 40, pp. 1528–1538, 1995.
- [4] J. A. Sethian, "A fast marching level set method for monotonically advancing fronts," in *Proc. Nat. Acad. Sci*, 1995, pp. 1591–1595.
- [5] G. Peyré, M. Pechaud, R. Keriven, and L. Cohen, "Geodesic methods in computer vision and graphics," *Foundations and Trends in Computer Graphics and Vision*, vol. 5, no. 3-4, pp. 197–397, 2010.
- [6] L. D. Cohen, "Multiple contour finding and perceptual grouping using minimal paths," *Journal of Mathematical Imaging and Vision*, vol. 14, no. 3, pp. 225–236, 2001.
- [7] F. Benmansour and L. D. Cohen, "Fast object segmentation by growing minimal paths from a single point on 2d or 3d images," *Journal of Mathematical Imaging and Vision*, vol. 33, no. 2, pp. 209–221, 2009.
- [8] —, "Tubular structure segmentation based on minimal path method and anisotropic enhancement," *International Journal of Computer Vision*, vol. 92, no. 2, pp. 192–210, Apr. 2011.
- [9] J.-M. Mirebeau, "Anisotropic fast-marching on cartesian grids using lattice basis reduction," *SIAM Journal on Numerical Analysis, Society for Industrial and Applied Mathematics*, vol. 52(4), pp. 1573–1599, 2014.
- [10] J. M. Mirebeau, "Efficient fast marching with finlser metrics," *Numerische Mathematik*, vol. 126, pp. 515–557, March 2014.
- [11] Y. Rouchdy and L. D. Cohen, "Geodesic voting for the automatic extraction of tree structures. methods and applications," *Computer Vision and Image Understanding*, vol. 117, no. 10, pp. 1453–1467, 2013.
- [12] —, "Retinal blood vessel segmentation using geodesic voting methods," in *Biomedical Imaging (ISBI), 2012, 9th IEEE International Symposium on*, May 2012, pp. 744–747.
- [13] —, "Geodesic voting methods: overview, extensions, and application to blood vessel segmentation," *Computer Methods in Biomechanics and Biomedical*

*Engineering: Imaging and Visualization*, vol. 1(2), pp. 79–88, June, 2013.